

***Original***

Thamburaja, P.; Klusemann, B.; Adibi, S.; Bargmann, S.:  
**The plastic yield and flow behavior in metallic glasses**  
In: Applied Physics Letters (2015) AIP

DOI: 10.1063/1.4907398

## The plastic yield and flow behavior in metallic glasses

Prakash Thamburaja,<sup>1,a)</sup> Benjamin Klusemann,<sup>2,b)</sup> Sara Adibi,<sup>3,c)</sup>  
 and Swantje Bargmann<sup>2,4,d)</sup>

<sup>1</sup>Department of Mechanical and Materials Engineering, National University of Malaysia (UKM),  
 Bangi 43600, Malaysia

<sup>2</sup>Institute of Continuum Mechanics and Material Mechanics, Hamburg University of Technology,  
 Eißendorfer Str. 42, 21073 Hamburg, Germany

<sup>3</sup>Department of Mechanical Engineering, National University of Singapore, BLK EA, #03-19S,  
 9 Engineering Drive 1, Singapore 117576, Singapore

<sup>4</sup>Institute of Materials Research, Helmholtz-Zentrum Geesthacht, Max-Planck-Straße 1, 21502 Geesthacht,  
 Germany

(Received 18 November 2014; accepted 21 January 2015; published online 4 February 2015)

Metallic glasses have vast potential applications as components in microelectronics- and nanoelectronics-type devices. The design of such components through computer simulations requires the input of a faithful set of continuum-based constitutive equations. However, one long-standing controversial issue in modeling the plastic behavior of metallic glasses at the continuum level is the use of the most appropriate plastic yield criterion and flow rule. Guided by a series of molecular dynamics simulations conducted at low-homologous temperatures under homogeneous deformations, we quantitatively prove that the continuum plastic behavior in metallic glasses is most accurately described by a von Mises-type plastic yield criterion and flow rule. © 2015 Author(s). All article content, except where otherwise noted, is licensed under a Creative Commons Attribution 3.0 Unported License. [<http://dx.doi.org/10.1063/1.4907398>]

Metallic glasses are metals which have an amorphous structure, and they are void of defects such as dislocations which weaken conventional crystalline metals. The ability to perform net-shape forming of components with very fine features make metallic glasses a suitable candidate for applications in the micro-electro-mechanical systems (MEMS), nano-electro-mechanical systems (NEMS), data storage, and biomedical equipment industries.<sup>1,2</sup>

From a continuum-based modeling perspective, one important issue which is still unresolved is the appropriate plastic yield criterion and flow rule which governs the behavior of metallic glasses. Experimental investigations of Pd and Zr-based metallic glasses<sup>3–5</sup> have shown that these are governed by either the von Mises or Mohr–Coulomb yield criterion. The discrepancy in these experimental findings is probably due to the insufficient size of the test samples. At low-homologous temperatures, one example of experiments on bulk Zr-based metallic glass samples was performed by Bruck *et al.*<sup>6</sup> suggesting that metallic glasses are governed by the von Mises yield criterion. Additionally, at low-homologous temperatures, the big drawback in ascertaining the appropriate yield criterion through experimental effort is due to the difficulty in determining the actual yield point of metallic glasses, since the samples easily undergo inhomogeneous deformations and shear banding/localization.<sup>7</sup>

Computationally, the yield behavior in metallic glasses was investigated in, e.g., Schuh and Lund<sup>8</sup> through a series of *molecular statics* simulations. From their results, Schuh and Lund<sup>8</sup> argue that metallic glasses are governed by the

Mohr–Coulomb plastic yield criterion. Yet, Ruan *et al.*<sup>9</sup> have shown that with the right values of material parameters, a Drucker–Prager (or pressure-sensitive von Mises) plastic yield criterion is also able to accurately reproduce the yield locus determined from Schuh and Lund.<sup>8</sup> The Mohr–Coulomb<sup>10</sup> model is able to accurately predict the experimentally observed shear band orientations in metallic glass samples under different loading conditions, e.g., simple tension/compression, plane-strain tension/compression, indentation, etc. However, the pressure-sensitive von Mises models of Zhao and Li<sup>11</sup> and Ruan *et al.*<sup>9</sup> are also able to accurately reproduce the shear band orientations under the same loading conditions. In their work, Zhao and Li<sup>11</sup> and Ruan *et al.*<sup>9</sup> also provide physical reasons to justify their choice of using a Mises-type yield criterion and flow rule to model the plastic behavior of metallic glasses. Recently, data obtained from molecular dynamics (MD) simulations based on a Dzugotov potential have shown that the plastic yield in metallic glasses is governed by a Mohr–Coulomb criterion.<sup>12</sup>

Hence, in our opinion, the issue of the appropriate plastic yield criterion and flow rule which best describes the plastic behavior of metallic glasses is still unresolved.

To resolve this issue, we will conduct our own molecular dynamics simulations for selected boundary value problems, and use the stress-strain data obtained from these simulations.

To ascertain the suitable continuum plastic yield criterion and flow rule which governs metallic glass behavior, we set out to determine the stress-strain responses of the Cu<sub>46</sub>Zr<sub>47</sub>Al<sub>7</sub> metallic glass system<sup>13</sup> in uniaxial tension/compression and plane-strain tension/compression via MD simulations. The Cu<sub>46</sub>Zr<sub>47</sub>Al<sub>7</sub> metallic glass system has a glass transition temperature,  $\theta_g \approx 700$  K.<sup>14</sup>

In the numerical experiments, starting with an amorphous structure, the Cu<sub>46</sub>Zr<sub>47</sub>Al<sub>7</sub> samples were heated up

<sup>a)</sup>Electronic mail: prakash.thamburaja@gmail.com

<sup>b)</sup>Electronic mail: benjamin.klusemann@tuhh.de

<sup>c)</sup>Electronic mail: sara.adibi@gmail.com

<sup>d)</sup>Electronic mail: swantje.bargmann@tuhh.de



from 300 K to 2500 K and then cooled down at a constant cooling rate of  $\dot{\theta}_c$  to the testing temperature of  $\theta_t \ll \theta_g$ . The MD simulations were performed within an NPT ensemble, and the temperature was controlled using the Nose-Hoover thermostat.

It is more convenient to determine the true state of stress at an *arbitrary* material point within a sample if the sample is deforming homogeneously. Since metallic glass specimens have a strong propensity to form shear bands during testing at low-homologous temperatures, special steps were taken to prepare the metallic glass samples so that they will only undergo *homogeneous* deformations in the simulations, and these include: (a) choosing an appropriate sample cooling rate  $\dot{\theta}_c$  so that prior to testing, the samples have an initial free volume which is significantly higher than the fully annealed free volume at test temperature  $\theta_t$ , and (b) deforming the samples at a temperature  $\theta_t$  which is not too low. For our numerical experiments, we have chosen  $\dot{\theta}_c = 1$  K/ps and  $\theta_t = 300$  K. Appropriate periodic boundary conditions are also applied on the samples so that shear offsets would not develop in the samples.

Uniaxial tension/compression loading is applied at a constant absolute strain rate of  $\dot{\epsilon} = 4 \times 10^8 \text{ s}^{-1}$ . For plane-strain loading, the deformation is applied at a constant absolute strain rate of  $\dot{\epsilon} = 2\sqrt{3} \times 10^8 \text{ s}^{-1}$  in order to ensure that the same rate effect is studied under both types of deformation. In the case of plane-strain loading, the deformation is additionally constrained in one direction. For more information regarding the MD simulations and sample preparation technique, please refer to the supplementary material.<sup>15</sup>

Figure 1 shows the initially undeformed cube-shaped amorphous metallic glass sample after the cooling process used in the MD simulations of the mechanical testing, and it comprises of 700 000 atoms. The sample has initial dimensions of 23 nm by 23 nm by 23 nm. The MD simulations were performed until a perfectly plastic stress-strain response is obtained, i.e., steady-state conditions are achieved.

Note that previous studies<sup>8,12</sup> use the yield point in their stress analysis to determine the appropriate yield criterion for metallic glasses in which the yield point is determined by the use of the strain offset method.<sup>16</sup> This method is

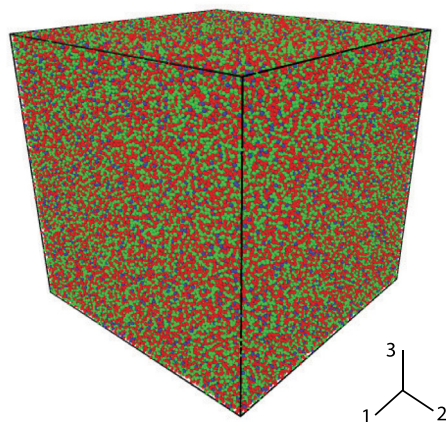


FIG. 1. Initial MD  $\text{Cu}_{46}\text{Zr}_{47}\text{Al}_7$  sample. Initially undeformed cube-shaped  $\text{Cu}_{46}\text{Zr}_{47}\text{Al}_7$  metallic glass sample consisting of  $\sim 700\,000$  atoms used in the molecular dynamics simulations (color code: green = Cu atoms, red = Zr atoms, and blue = Al atoms).

generally used to determine the yield point of metallic glasses because the transition from elastic to elastic-plastic deformation is very smooth and not very discernable from the stress-strain response. To circumvent the shortcomings<sup>12</sup> of the strain offset method, we choose to use the stress data at steady-state flow in our subsequent analysis because its value can be very easily determined from the stress-strain data. Furthermore, unlike the yield point or peak stress level, the steady-state stress value is *insensitive* to sample preparation conditions such as annealing time, cooling rate, etc., cf. the experiments in Ref. 17 and supplementary Figure S2.<sup>15</sup>

Figure 2 shows the absolute-valued stress-strain curves for the  $\text{Cu}_{46}\text{Zr}_{47}\text{Al}_7$  metallic glass system in uniaxial tension/compression and plane-strain tension/compression at 300 K under *isothermal* conditions. For the uniaxial tension/compression simulations, only the applied (or loading) stress response is shown, whereas the loading and constraint stress responses are shown for the plane-strain tension/compression simulations. From the perfectly plastic (or steady-state) stress-strain responses shown in Figure 2 (whose values are tabulated in Table I as well as in detail in supplementary Table SI<sup>15</sup> for convenience), two very important trends are observed:

- **Trend 1:** The loading stress in plane-strain tension/compression is *markedly* different and higher than the loading stress in uniaxial tension/compression.
- **Trend 2:** The constraint stress in plane-strain tension/compression is very close to one-half of the loading stress in plane-strain tension/compression.

It is worth noticing that the obtained tension-compression asymmetry of 7%–9% in the molecular dynamic simulations of the  $\text{Cu}_{46}\text{Zr}_{47}\text{Al}_7$  metallic glass system agrees well with experimental observed tension-compression asymmetries in the range of 7%–10% for different metallic glass systems.<sup>18–20</sup>

Generally, the plastic flow rule associated with the pressure-sensitive von Mises yield criterion is called the von Mises plastic flow rule, whereas the plastic flow rule associated with the Mohr–Coulomb yield criterion is referred to as the double-shear plastic flow rule.<sup>10</sup>

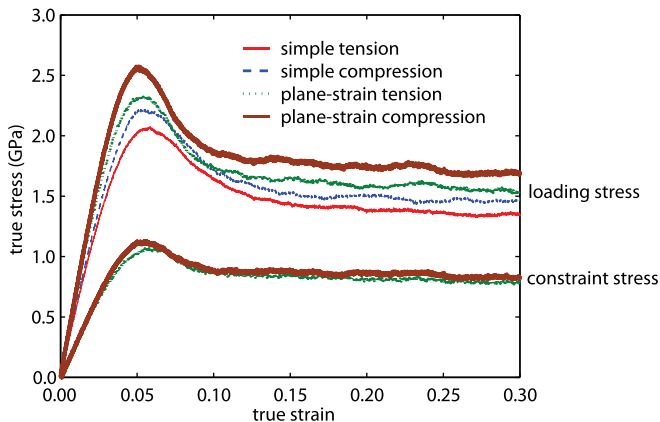


FIG. 2. Stress-strain curves. The absolute-valued stress-strain curves in simple tension, simple compression, plane-strain tension, and plane-strain compression for a  $\text{Cu}_{46}\text{Zr}_{47}\text{Al}_7$  metallic glass system at 300 K. A perfectly plastic stress-strain response is obtained, i.e., steady-state conditions are achieved.

TABLE I. The steady-state stresses obtained from the MD simulations. Further, the theoretical steady-state stresses determined from the von Mises plastic yield criterion and flow rule and the Mohr–Coulomb yield criterion and the double-shear plastic flow rule are listed. The former predicts the stress results obtain from MD simulations very well, whereas the latter does not map them. Notation:  $L$ : loading stress;  $C$ : constraint stress;  $r = C/L$ : ratio of constrained to loading stress; NA: not applicable; and ID: indeterminable.

	Cu <sub>46</sub> Zr <sub>47</sub> Al <sub>7</sub> metallic glass system								
	Molecular dynamics			von Mises			Mohr–Coulomb		
	$L_{MD}$	$C_{MD}$	$r_{MD}$	$L_{VM}$	$C_{VM}$	$r_{VM}$	$L_{MC}$	$C_{MC}$	$r_{MC}$
ST	1.36 GPa	NA	NA	1.36 GPa	NA	NA	1.36 GPa	NA	NA
SC	−1.46 GPa	NA	NA	−1.46 GPa	NA	NA	−1.46 GPa	NA	NA
PST	1.56 GPa	0.80 GPa	0.51	1.53 GPa	0.76 GPa	0.5	1.36 GPa	ID	ID
PSC	−1.70 GPa	−0.83 GPa	0.49	−1.73 GPa	−0.87 GPa	0.5	−1.46 GPa	ID	ID

In the next paragraph, the suitability of a pressure-sensitive von Mises plastic yield criterion and a von Mises plastic flow rule versus a Mohr–Coulomb yield criterion and a double-shear plastic flow rule, in *quantitatively* verifying trends 1 and 2, is discussed.

The material parameters in the von Mises and Mohr–Coulomb yield criteria are fitted to the uniaxial tension and compression data from the molecular dynamic simulations, whereas the data obtained from the plane-strain tension and compression simulations are used for independent prediction.

With integers  $\alpha = 1, 2, 3$ , let  $T_\alpha$ ,  $D_\alpha$ , and  $D_\alpha^p$  denote the principal values of the Cauchy stress, total stretching rate, and plastic distortion rate, respectively, along principal axis  $\alpha$ . Principal axis 1 represents the loading direction. For the plane-strain tension/compression cases, principal axes 2 and 3 represent the constraint and free directions, respectively. For simplicity, we assume that the deformation is *isochoric*, i.e.,  $D_1 + D_2 + D_3 = 0$ . The analysis performed is restricted to homogeneous deformations of the sample.

From experimental data, it is ascertained that the deformation behavior of metallic glasses at temperatures well below the glass transition temperature is virtually rate-insensitive over a broad range of strain rates.<sup>21,22</sup> Therefore, we obtain the following pressure-sensitive von Mises (or Drucker–Prager) plastic yield criterion by taking the rate-dependent plastic shear strain kinetic equation of Thamburaja<sup>23</sup> and Bargmann *et al.*<sup>24</sup> in the rate-independent limit

$$\bar{\tau} - \zeta \bar{p} = s, \quad (1)$$

where the equivalent shear stress

$$\bar{\tau} = \sqrt{1/6([T_1 - T_2]^2 + [T_2 - T_3]^2 + [T_3 - T_1]^2)} \geq 0, \quad (2)$$

and the hydrostatic pressure  $\bar{p} = -1/3 [T_1 + T_2 + T_3]$ . The quantity  $s = \hat{s}(\text{free volume}) > 0$  denotes the total resistance to plastic deformation, and  $\zeta$  is the free volume creation coefficient. Equation (1) reduces to the classical von Mises yield criterion if  $\zeta = 0$ .

For the simple tension/compression cases,  $T_2 = T_3 = 0$  holds. Substitution into Eq. (1) yields

$$\frac{1}{\sqrt{3}} |T_1| + \frac{\zeta}{3} T_1 = s. \quad (3)$$

The values for the free volume creation coefficient  $\zeta$  and the total resistance to plastic deformation  $s$  at steady-state are

obtained by substituting the values of the MD-determined steady-state stresses in simple tension and compression (see Table I) into Eq. (3), leading to  $\zeta = 0.062$  and  $s = 0.812$  GPa.

In the case of plane-strain tension/compression, we have  $T_3 = 0$  and  $D_2 = 0$ . During steady-state response, there are no elastic distortions, i.e.,  $D_\alpha = D_\alpha^p$  for  $\alpha = 1, 2, 3$ . For a material which is governed by a pressure sensitive von Mises plastic flow rule, the principal values for the plastic distortion rate under *steady-state* conditions are given by

$$D_\alpha^p = \frac{\dot{\gamma}}{2\bar{\tau}} [T_\alpha + \bar{p}] = D_\alpha, \quad \alpha = 1, 2, 3, \quad (4)$$

see Refs. 23 and 24. The quantity

$$\dot{\gamma} = \sqrt{2/3 [(D_1^p - D_2^p)^2 + (D_2^p - D_3^p)^2 + (D_3^p - D_1^p)^2]} \geq 0, \quad (5)$$

represents the plastic shearing rate. Thus, we obtain

$$D_2^p = \frac{\dot{\gamma}}{6\bar{\tau}} [2T_2 - T_1] = D_2 = 0 \Rightarrow T_2 = \frac{1}{2} T_1, \quad (6)$$

for the plane-strain tension/compression cases, since  $\dot{\gamma} > 0$  and  $\bar{\tau} > 0$  during plastic deformation. Hence, under *steady-state* plane-strain conditions, the constraint stress is always one-half of the loading stress for a material governed by a von Mises plastic flow rule. This agrees very well with the results of our MD simulations for the plane-strain tension/compression cases, cf. Table I.

Finally, the loading stress  $T_1$  and the constraint stress  $T_2$  for the plane-strain tension/compression cases at *steady-state* are calculated by substituting  $T_2 = 1/2 T_1$  and  $T_3 = 0$  into Eq. (1)

$$T_1 = \pm \frac{2s}{1 \pm \zeta}, \quad T_2 = \frac{1}{2} T_1 = \pm \frac{s}{1 \pm \zeta}, \quad (7)$$

where the + sign is for plane-strain tension and the − sign is for plane-strain compression. For the plane-strain tension/compression cases, the values of the loading ( $L_{VM}$ ) and constraint stresses ( $C_{VM}$ ) under *steady-state* conditions are obtained by substituting  $\zeta = 0.062$  and  $s = 0.812$  GPa into Eq. (7):  $L_{VM} = 1.53$  GPa and  $C_{VM} = 0.76$  GPa (plane-strain tension),  $L_{VM} = -1.73$  GPa and  $C_{VM} = -0.87$  GPa (plane-strain compression).

The values of the steady-state stresses in simple tension/compression and plane-strain tension/compression obtained by the Mohr–Coulomb plastic yield criterion and the

double-shear plastic flow rule are also presented in Table I. Since the intermediate principal stress has no effect on the applied stress required to cause plastic yielding,<sup>5,25</sup> the value of the steady-state loading stress in the plane-strain tension/compression case ( $L_{MC, PST}$ ,  $L_{MC, PSC}$ ) is equal to the value of the steady-state loading stress in the simple tension/compression case ( $L_{MC, ST}$ ,  $L_{MC, SC}$ ) for a material governed by a Mohr–Coulomb plastic yield criterion (see also Ref. 8). Thus, the predictions from the Mohr–Coulomb plastic yield criterion clearly violate trend 1 of the MD simulation results.

Furthermore, the steady-state constraint stress ( $C_{MC}$ ) in the plane-strain tension/compression case is indeterminable by the Mohr–Coulomb yield criterion and the double-shear plastic flow rule. This artifact is due to the inherent characteristics of the Mohr–Coulomb yield criterion and the double-shear plastic flow rule, i.e., the plastic flow direction in the double-shear plastic flow rule depends on a material parameter termed as the *angle of internal friction*.<sup>10</sup> Hence, the Mohr–Coulomb yield criterion and the double-shear plastic flow rule associated with it are also unable to ascertain the special relationship between the constraint stress and the loading stress for steady-state stress-strain responses under plane-strain conditions, i.e., trend 2 of the MD simulation results. These results are confirmed for two further alloy systems as well. The stress-strain curves are shown in supplementary Figures S3 and S4, and the results are summarized in supplementary Tables SI and SII<sup>15</sup> for convenience.

The pressure-sensitive von Mises yield criterion and the von Mises plastic flow rule very accurately *predict* the level of loading and constraint stresses seen in the plane-strain tension/compression MD simulations *quantitatively*. In contrast, the Mohr–Coulomb yield criterion does not map the steady-state loading stresses for the plane-strain tension/compression cases. Furthermore, the constraint stresses for the plane-strain tension/compression cases are indeterminable due to the inherent nature of the Mohr–Coulomb-type yield criterion and the double-shearing plastic flow rule.

Hence, from the MD simulations in simple tension, simple compression, plane-strain tension and plane-strain

compression, it is ascertained that the use of a pressure-sensitive von Mises yield criterion and a von Mises plastic flow rule is more appropriate to accurately describe the plastic yield and flow behavior in metallic glasses, respectively.

P.T. acknowledges the financial support provided by the Arus Perdana program of UKM under Grant No. AP-2012-022. Part of this research was done while P.T. visited Hamburg University of Technology, Germany.

- <sup>1</sup>J. Schroers, *JOM* **57**, 35 (2005).
- <sup>2</sup>G. Kumar, A. Desai, and J. Schroers, *Adv. Mater.* **23**, 461 (2011).
- <sup>3</sup>H. Kimura and T. Matsumoto, *Amorphous Metallic Alloys* (Butterworths, London, 1983).
- <sup>4</sup>P. Donovan, *Mater. Sci. Eng.* **98**, 487 (1988).
- <sup>5</sup>P. Donovan, *Acta Metall.* **37**, 445 (1989).
- <sup>6</sup>H. Bruck, T. Christian, A. Rosakis, and W. Johnson, *Scr. Metall. Mater.* **30**, 429 (1994).
- <sup>7</sup>R. Schwarz, "Bulk Amorphous Alloys," in *Intermetallic Compounds - Principles and Practice: Progress, Volume 3*, edited by J. H. Westbrook and R. L. Fleischer (John Wiley & Sons Ltd), Chap. 32, pp. 681–705.
- <sup>8</sup>C. Schuh and A. Lund, *Nat. Mater.* **2**, 449 (2003).
- <sup>9</sup>H. Ruan, L. Zhang, and J. Lu, *Int. J. Solids Struct.* **48**, 3112 (2011).
- <sup>10</sup>L. Anand and C. Su, *J. Mech. Phys. Solids* **53**, 1362 (2005).
- <sup>11</sup>M. Zhao and M. Li, *Appl. Phys. Lett.* **93**, 241906 (2008).
- <sup>12</sup>M. Vargonen, L. Huang, and Y. Shi, *J. Non-Cryst. Solids* **358**, 3488 (2012).
- <sup>13</sup>Y. Q. Cheng, E. Ma, and H. W. Sheng, *Phys. Rev. Lett.* **102**, 245501 (2009).
- <sup>14</sup>D. Xu, G. Duan, and W. L. Johnson, *Phys. Rev. Lett.* **92**, 245504 (2004).
- <sup>15</sup>See supplementary material at <http://dx.doi.org/10.1063/1.4907398> for further details on the set-up of the MD simulations, sample preparation techniques as well as results for additional alloy systems.
- <sup>16</sup>J. Rottler and M. Robbins, *Phys. Rev. E* **64**, 051801 (2001).
- <sup>17</sup>P. De Hey, J. Sietsma, and A. van den Beukel, *Acta Mater.* **46**, 5873 (1998).
- <sup>18</sup>G. He, J. Lu, Z. Bian, D. Chen, G. Chen, G. Tu, and G. Chen, *Mater. Trans.* **42**, 356 (2001).
- <sup>19</sup>T. Mukai, T. Nieh, Y. Kawamura, A. Inoue, and K. Higashi, *Intermetallics* **10**, 1071 (2002).
- <sup>20</sup>Z. Zhang, J. Eckert, and L. Schultz, *Acta Mater.* **51**, 1167 (2003).
- <sup>21</sup>H. Bruck, A. Rosakis, and W. Johnson, *J. Mater. Res.* **11**, 503 (1996).
- <sup>22</sup>J. Lu, G. Ravichandran, and W. Johnson, *Acta Mater.* **51**, 3429 (2003).
- <sup>23</sup>P. Thamburaja, *J. Mech. Phys. Solids* **59**, 1552 (2011).
- <sup>24</sup>S. Bargmann, T. Xiao, and B. Klusemann, *Philos. Mag.* **94**, 1 (2014).
- <sup>25</sup>M. Jirasek and Z. Bazant, *Inelastic Analysis of Structures* (Wiley, 2001).